Developmental Biology 327 (2009) 313–326

Contents lists available at ScienceDirect

Developmental Biology

journal homepage: www.elsevier.com/developmentalbiology

EphA4 and EfnB2a maintain rhombomere coherence by independently regulating intercalation of progenitor cells in the zebrafish neural keel

Hilary A. Kemp, Julie E. Cooke [1], Cecilia B. Moens *

Howard Hughes Medical Institute and Division of Basic Science, Fred Hutchinson Cancer Research Center, B2-152, 1100 Fairview Ave. N., Seattle WA 98109, P.O. Box 19024, USA

ARTICLE INFO

Article history:
Received for publication 14 August 2008
Revised 6 December 2008
Accepted 10 December 2008
Available online 24 December 2008

Keywords:
Eph
Ephrin
Efn
Hindbrain
Boundary
Zebrafish
Rhombomere
Neuroepithelium
Cell affinity
Cell sorting

ABSTRACT

During vertebrate development, the hindbrain is transiently segmented into 7 distinct rhombomeres (r). Hindbrain segmentation takes place within the context of the complex morphogenesis required for neurulation, which in zebrafish involves a characteristic cross-midline division that distributes progenitor cells bilaterally in the forming neural tube. The Eph receptor tyrosine kinase EphA4 and the membrane-bound Ephrin (Efn) ligand EfnB2a, which are expressed in complementary segments in the early hindbrain, are required for rhombomere boundary formation. We showed previously that EphA4 promotes cell–cell affinity within r3 and r5, and proposed that preferential adhesion within rhombomeres contributes to boundary formation. Here we show that EfnB2a is similarly required in r4 for normal cell affinity and that EphA4 and EfnB2a regulate cell affinity independently within their respective rhombomeres. Live imaging of cell sorting in mosaic embryos shows that both proteins function during cross-midline cell divisions in the hindbrain neural keel. Consistent with this, mosaic EfnB2a over-expression causes widespread cell sorting and disrupts hindbrain organization, but only if induced at or before neural keel stage. We propose a model in which Eph and Efn-dependent cell affinity within rhombomeres serve to maintain rhombomere organization during the potentially disruptive process of teleost neurulation.

Introduction

The ability of cells to make adhesive contacts with appropriate neighbours, while avoiding others, is a fundamental process that underlies development as well as adult function in multicellular animals, and relies on cell surface determinants that allow cells to identify one another. In the vertebrate hindbrain, which is divided into seven segments or rhombomeres, experimental juxtaposition of cells with different segment identities results in their robust sorting-out (Cooke et al., 2005; Guthrie and Lumsden, 1991; Guthrie et al., 1993; Moens et al., 1996; Waskiewicz et al., 2002; Xu et al., 1999). These cell behaviours are thought to underlie the establishment and maintenance of rhombomere boundaries during normal neuroepithelial development.

Mechanistically, cell sorting has been shown to be driven efficiently by either repulsion between unlike cells or differential adhesion between like cells. The Eph receptor tyrosine kinases and their Ephrin (Efn) ligands are membrane proteins that mediate cell–cell repulsion and attraction in many developmental contexts (Egea and Klein, 2007; Hirashima and Suda, 2006; Klein, 2004; Poliakov et al., 2004; Sela-Donenfeld and Wilkinson, 2005). The outcome of a given Eph–Ephrin interaction is context-dependent, and both in vivo and in vitro, receptor–ligand pairs have been shown to mediate cell–cell repulsion in some instances, while promoting adhesion in others (Eberhart et al., 2004; Hindges et al., 2002; McLaughlin et al., 2003; Santiago and Erickson, 2002).

In the developing zebrafish hindbrain, EphA4 is expressed in rhombomeres 3 and 5 while EfnB ligands EfnB2a and EfnB3 are expressed in the adjacent rhombomeres (Bergemann et al., 1995; Chan et al., 2001; Nieto et al., 1992). Knock-down of EphA4 results in the loss of rhombomere boundaries and the disruption of normal segmental hindbrain neuroanatomy, a phenotype that is exacerbated by simultaneous depletion of EfnB2a, consistent with a critical role for these molecules in regulating the cell sorting behaviours that drive rhombomere boundary formation and maintenance (Cooke et al., 2005). Initial over-expression experiments in which EphA4-over-expressing cells sorted out from EfnB2a-expressing rhombomeres and vice versa suggested that the underlying cell sorting mechanism was mutual cell repulsion driven by Eph–Ephrin interactions at boundaries (Mellitzer et al., 1999; Xu et al., 1999). However by mosaic analysis using loss-of-function reagents we discovered that cells lacking EphA4 sort out from cells expressing EphA4 in r3 and r5 where EfnB2a is not expressed, suggesting that the EphA4 protein has an EfnB2a-independent adhesive role within the forming r3 and r5 territories

* Corresponding author. Division of Basic Science, Fred Hutchinson Cancer Research Center, B2-152, 1100 Fairview Ave. N., Seattle WA 98109, P.O. Box 19024, USA.
E-mail address: cmoens@fhcrc.org (C.B. Moens).
[1] Current address: Summit plc, 91 Milton Park, Abingdon, Oxfordshire, OX14 4RY, UK.

0012-1606/$ – see front matter © 2009 Elsevier Inc. All rights reserved.
doi:10.1016/j.ydbio.2008.12.010

(Cooke et al., 2005). Here we describe a corresponding EphA4-independent requirement for the EfnB2a ligand in regulating cell affinity between cells within rhombomere 4 (r4).

Sharpening of rhombomere boundaries in teleosts coincides with the complex morphogenetic movements required for neurulation. Previously we have shown that EphA4-based sorting in mosaic embryos begins in the neural keel (Cooke et al., 2005), an intermediate stage in neurulation characterized by cross-midline cell divisions that generate bilateral clones (Kimmel et al., 1994; Papan and Campos-Ortega, 1999). In this work, we identify the cellular behaviors regulated by EphA4 and EfnB2a in the context of this morphogenesis. Using time-lapse analysis of cell sorting in mosaic embryos, we find that EphA4 and EfnB2a are specifically and individually required to facilitate normal integration of newborn progenitor cells during the cross-midline cell division that occurs at the neural keel/rod stage in zebrafish neurulation. We propose a model in which both EphA4 and EfnB2a are required for rhombomere-specific cell affinity and thus to maintain rhombomere coherence and bilateral symmetry during the

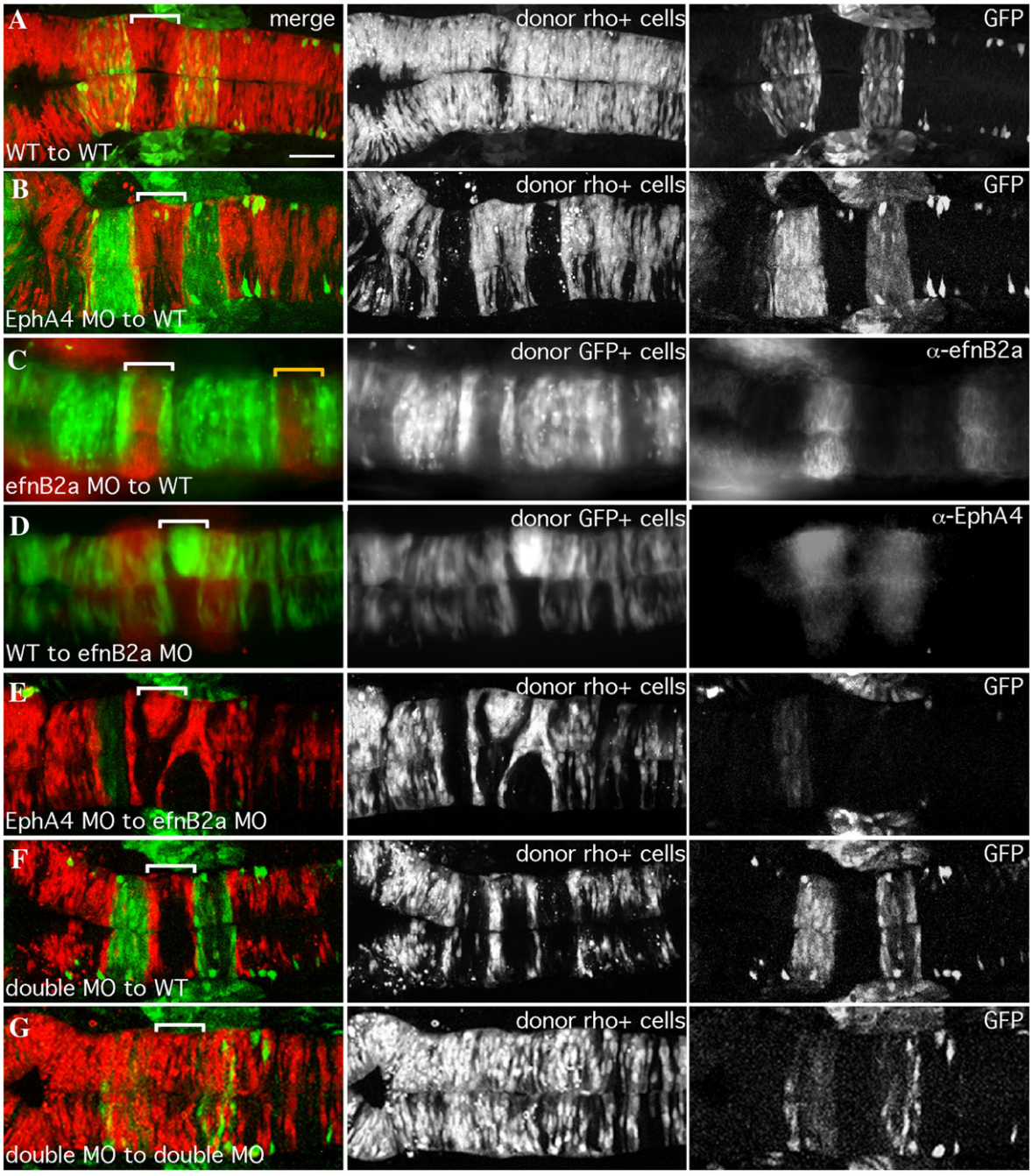

Fig. 1. EfnB2a promotes cell adhesion in r4 independent of EphA4. 18 hpf mosaic embryos shown in dorsal view with anterior to the left. Left panels are merged images of individual channels shown in the middle and right panels. Donor cells (middle panel), are labeled with rhodamine dye (red in the merge; A, B, E, F, G) or express GFP (green in the merge; C, D). Rhombomere-specific markers (right panel): r3 and r5 are identified by expression of GFP in pGFP5.3 transgenic hosts (green in the merge; A, B, E, F, G) or detected by α-EphA4 (red in the merge; D); α-EfnB2a marks r1, r4, r7 (red in the merge; C). r4 is indicated by a white bracket in the merge. (A) WT cells contribute evenly to a WT host hindbrain. (B) EphA4 MO donor cells are excluded from r3 and r5 of a WT host. (C) EfnB2a MO donor cells are excluded from r4 and r7 (yellow bracket) of a WT host embryo. (D) WT donor cells form unilateral clusters on one side of r4 of an EfnB2a MO host. (E) EphA4 MO donor cells are excluded from r3 and r5 and form a unilateral cluster in r4 of an EfnB2a MO host embryo. (F) EfnB2a; EphA4 double MO donor cells are excluded from r3, r4, and r5 of WT host embryos. (G) EphA4; EfnB2a double MO donor cells contribute homogeneously to the hindbrain of a double MO host embryo. Scale bar: 50 μm.

Table 1
Summary of EphA4 and EfnB2a MO mosaic analyses

Donor	Host			
	Uninjected	EphA4MO	EfnB2aMO	EphA4MO; EfnB2aMO
Uninjected	Throughout hindbrain (*N*=41)	Cluster in r3, r5 (*N*=47)	Cluster in r4 (*N*=27)	Cluster in r3,r4,r5 (*N*=53)
EphA4MO	Sort from r3, r5 (*N*=95)	Throughout hindbrain (*N*=9)	Cluster in r4; sort from r3, r5 (*N*=13)	N/D
EfnB2aMO	Sort from r4 (*N*=97)	Cluster in r3, r5; sort from r4 (*N*=8)	Throughout hindbrain (*N*=11)	N/D
EphA4MO; EfnB2aMO	Sort from r3, r4, r5 (*N*=10)	N/D	N/D	Throughout hindbrain (*N*=12)

The distribution of uninjected or morphant (MO) donor cells (left column) transplanted into uninjected or MO (top row) host embryos is indicated. Notably, MO donor cells contribute homogeneously to hindbrains of hosts treated with an identical combination of MO(s) and segregate from host cells in specific rhombomeres when transplanted into hosts treated with a different combination of MO(s). Furthermore, phenotypes observed in one combination of MO to WT transplant (or vice versa) are additive when multiple MO combinations are used. N/D (not done).

potentially disruptive cross-midline divisions that serve to extend the teleost neuraxis.

Materials and methods

Dye, morpholino and nucleic acid injections

1-cell stage zebrafish embryos were injected with 1 nl of fixable rhodamine dye, morpholino (MO), or nucleic acid. MO preparation was as described previously (Cooke et al., 2005). Plasmid DNA or capped mRNA synthesized with mMESSAGE mMACHINE (Ambion) was resuspended in nuclease-free water (Ambion). Morpholinos were as follows: EphA4TB, 5 μg/μl (Cooke et al., 2005); EfnB2aTB MO-2 AATATCTCCACAAAGAGTCGCCCAT, 3 μg/μl (Koshida et al., 2005). Identical phenotypes to those reported here were also obtained with EfnB2aTB MO-1, 10 μg/μl (Cooke et al., 2005). mRNAs were as follows: WT EphA4 from pCS-EphA4 (Cooke et al., 2005) at 300–600 ng/μl; EfnB2a WT and mutant alleles from pCS-EfnB2a and pCS-EfnB2a-ΔC-eGFP 1-200 ng/μl; GFP from pCS-eGFP at 100 ng/μl; membrane RFP (mRFP) at 100 ng/μl from pCS-memb-mRFP1 (Megason and Fraser, 2003); histone-GFP at 25 ng/μl from pCS-H2B-GFP (Kanda et al., 1998); transposase at 25 ng/μl from pCS2FA-TP (Kwan et al., 2007). The bidirectional heat shock vector, pHS-GFP-Tol2, was generously provided by D. Kimelman. Full-length EfnB2a and EfnB2a-ΔC were co-expressed with GFP by cloning into the non-GFP cassette of pHS-GFP-Tol2 and injected at 12 ng/μl. EphA4 and EfnB2a expression constructs were MO-resistant alleles, in which silent base pair changes were introduced.

RNA in situ hybridization and immunostaining

RNAs in situs were carried out as described (Prince et al., 1998) using a *krox20*/*egr2b* riboprobe (Oxtoby and Jowett, 1993). Plastic sections of RNAs in situ were made as described (Westerfield, 1993). Whole mount immunostaining was performed as described (Cooke et al., 2005), except some embryos that were fixed in 4% paraformaldehyde for only 3 h at room temperature to preserve GFP or mRFP fluorescence. Primary antibodies were as follows: α-EphA4 (Upstate; 1:200); α-EfnB2a (R&D Biosystems, 1:100); α-aPKCζ (Santa Cruz C20, 1:500); α-laminin Ab-1 (NeoMarkers/ThermoScientific RB-082-A1; 1:100); α-3A10 (DHSBank; 1:200) α-HU (Invitrogen; 1:200). Secondary antibodies were fluorochrome-conjugated Alexa Fluor 488, 594, or 633 (Invitrogen).

Gastrula stage mosaic analysis and confocal imaging

Mosaics made by cell transplantation at early gastrula stages were performed as previously described (Carmany-Rampey and Moens, 2006). Confocal imaging was essentially as previously described (Cooke et al., 2005). For time-lapse imaging, embryos were mounted live at ~10 hpf in a drop of 0.6% low-melting-point agarose on a 35 mm coverglass-bottom culture dish (MatTek) and imaged for ~10 h at 30 °C on a heated stage attached to a Zeiss Pascal confocal inverted microscope. The phenotypes ascribed to each of the types of mosaics described in Fig. 1 and Table 1 were apparent in more than 75% of the mosaics generated in any given experiment. High-resolution confocal timelapse imaging of clump formation in WT to EphA4 MO mosaics was performed on 9 embryos over the course of 6 separate experimental trials; quantitation of cell position and spindle orientation during clump formation was performed on a representative embryo as described in Fig S7 and Table 2. Confocal timelapse imaging of EfnB2a MO cells sorting out of WT r4 was performed on 6 embryos in 2 separate trials. The movies shown in Figs. S2–4 consist of projected z-stacks at 15 min intervals extracted from time-lapses obtained using a 20× objective with a 1.3–1.5× zoom. Images in Fig. 2 are projections corresponding to a 30-μm-deep volume in the middle of the dorso-ventral axis of the zebrafish hindbrain. Images in Fig. 4 are individual confocal sections extracted from a time-lapse obtained using a 40× water immersion objective, and Immersol (Zeiss).

Neural rod stage transplants

Single cells or small groups of cells were transplanted from donor r3 to host r4 at the 10–12 somite stage (14–15 hpf) with a glass pipette with a 10–15 μm inner diameter using an oil-controlled micromanipulator mounted on a Zeiss Axioskop FSII fixed-stage microscope. Both donor and host embryos were from the pGFP5.3 transgenic line (Picker et al., 2002) which expresses GFP in r3 and r5. Donor embryos were injected at the 1-cell stage with biotin-conjugated dextran to visualize donor-derived cells after transplantation. Host embryos were imaged immediately after transplantation to confirm the location of donor-derived cells, and then were fixed 4–5 h after transplantation. *Krox20* expression was detected by RNA in situ hybridization followed by fluorescent detection of the biotin-dextran using the TSA kit (Molecular Probes, now Invitrogen). Donor cells in r4 were scored as "plastic" if they lacked *krox20* expression and "not plastic" if they still expressed *krox20*.

Quantitation of cell position and spindle orientation during cell divisions in the neuroepithelium

Cell divisions were observed over the course of the time-lapse described in Fig. 4. r3 and r5 were identified by GFP expression in the

Table 2
Characterization of donor cell divisions in a WT to EphA4 MO mosaic

(*t*)	(*r*)	(*N*)	Spindle orientation (mitosis)	Mother position (mitosis)	Daughter position (neural tube)
Keel	r4	24	100% apico-basal	92% medial	71% bilateral
	r3,5	36	75% apico-basal	81% lateral	100% unilateral
Tube	r4	11	82% planar	100% medial	100% unilateral
	r3,5	18	67% planar	72% lateral	100% unilateral

Cell divisions were observed over the course of the time-lapse described in Fig. 4. Dividing donor cells in the neural keel/rod and neural tube at the level of r3, r4 and r5 were scored for mediolateral nuclear position during mitosis, spindle orientation at the metaphase-to-anaphase transition, and the position of donor-derived daughter cells at neural tube stage. The behaviour of the majority of the cells at a given time/space coordinate is indicated as a percentage of total divisions scored (*N*). Underlined text indicates that a majority of cells (>50%) exhibit abnormal behaviour.

pGFP5.3 transgenic host embryo (Picker et al., 2002). It has previously been described that formation of the neural keel occurs between 6 and 10 s (12–14 hpf), transition into the neural rod is complete by 14 s (16 hpf) and the neural tube stage begins at 17–18 s (17 hpf) (Geldmacher-Voss et al., 2003). In our experiments, cross-midline division of donor cells in r4 were observed as early as 12.5 hpf, and planar divisions typical of neural tube stage were first observed at 17 hpf. The midline was defined as equidistant from each of the lateral surfaces of the neuroepithelium. Nuclear position of dividing cells was scored as medial if closer to the midline, and lateral if closer to the lateral edges of the neuroepithelium. Spindle orientation was assumed to be perpendicular to the plane of the metaphase plate. Divisions were scored as planar if the angle between the midline and the spindle at anaphase was less than 45°, and scored as apico-basal if the angle between the spindle and midline was more than 45°, consistent with previous criteria used to determine spindle orientation in chicken and zebrafish neuroepithelia (Geldmacher-Voss et al., 2003; Roszko et al., 2006). Final position of daughter cells was scored as bilateral if one daughter crossed the midline after mitosis and unilateral if both daughters remained on the same side.

Cell division inhibitors

To block cross-midline cell divisions, embryos were cultured from 90% epiboly onwards in embryo medium containing 100 μM aphidicolin (Sigma) and 20 mM hydroxyurea (Sigma) dissolved in 4% DMSO, as previously described (Tawk et al., 2007). Control embryos were treated with 4% DMSO.

Heat shock

Heat shock mosaics were generated by co-injection of 12 pg plasmid DNA and 25 pg transposase mRNA in a 1 nl volume; a subset of embryos was coinjected with EfnB2a MO. Embryos raised at 28 °C

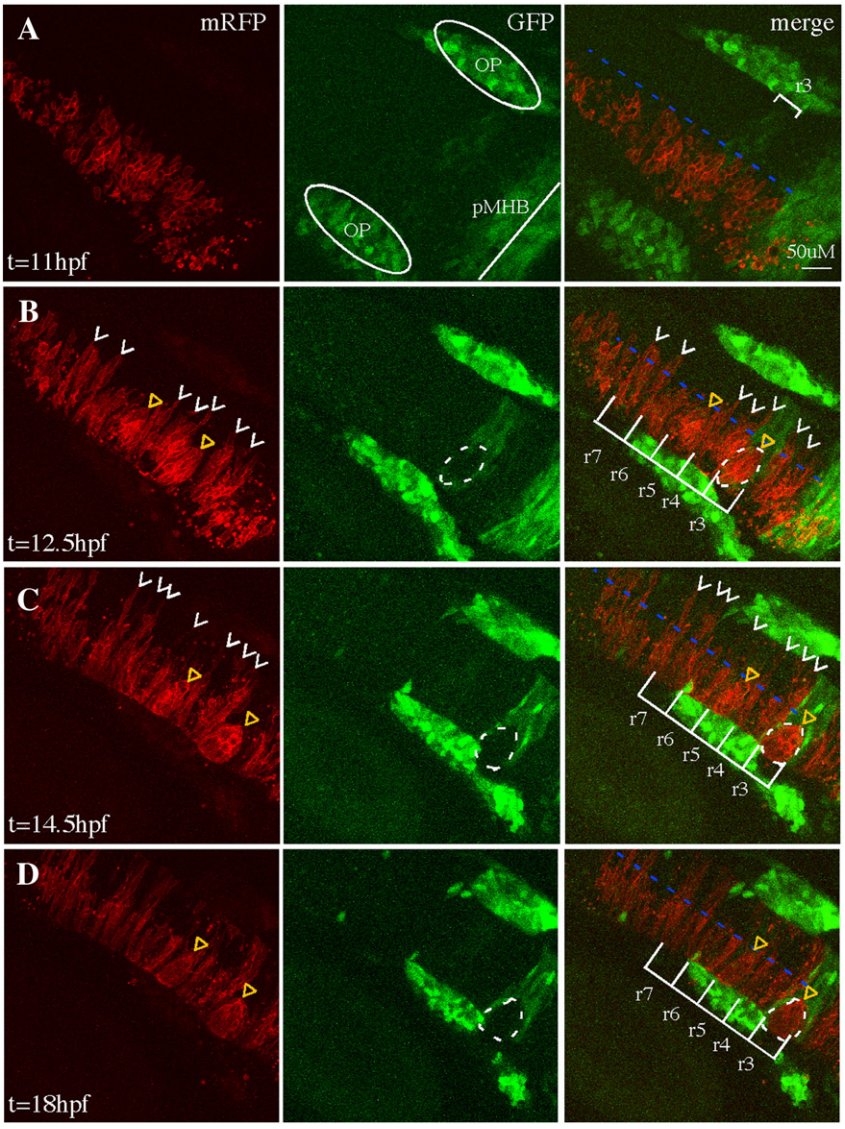

Fig. 2. Cell sorting in EphA4MO mosaics begins during the neural keel stage. Representative 30 μm-deep projections of adjacent confocal sections through the hindbrain of a live mosaic embryo are shown at the indicated time points. Left panel: distribution of mRFP+ WT donor cells. Middle panel: expression of GFP in r3, r5 of the EphA4 MO pGFP5.3 transgenic host. Right panel is a merge of two channels shown at left. (A) At 11 hpf (neural plate), cells are uniformly distributed on one side of the hindbrain. (B) At 12.5 hpf (neural keel), presumptive daughters of neural progenitor divisions (white arrowheads) have begun to cross the midline (blue dotted line) but none is observed crossing in the r3 or r5 interior. (C, D) By 14.5 hpf (neural rod) and 18 hpf (neural tube), many donor cells have successfully crossed the midline (white arrowheads) except in r3 and r5, where WT mRFP+, GFP− cells form unilateral cell clusters (yellow triangles). OP (otic placode); pMHB (presumptive midbrain–hindbrain boundary). Scale bar: 50 μm.

were heat shocked at 39 °C for 1 h, then returned to 28 °C. Phenotypes were observed at 18 hpf. Controls injected with identical reagents were incubated at 28 °C.

Results

EphA4 and EfnB2a are required independently to mediate normal intra-rhombomere cell interactions

Initial studies on EphA4 and EfnB2a function in hindbrain segmentation supported a role for these proteins in mutual cell repulsion at boundaries (Xu et al., 1999). Using morpholino (MO) knock-down we confirmed a requirement for EphA4 in rhombomere boundary formation; however we demonstrated using mosaic analysis that EphA4 promotes cell–cell affinity within r3 and r5 because EphA4 morphant (MO) cells sort out from wild type (WT) EphA4+ cells within r3 or r5 where EphA4 is expressed. Specifically, EphA4-depleted cells are sorted out of WT r3 and r5 while WT cells form unilateral clusters in r3 and r5 of an EphA4 MO host (Fig. 1B and Cooke et al., 2005). EfnB2a is not expressed in r3 and r5, and EphA4 knock-down did not result in up-regulation of EfnB2a, so these sorting behaviours cannot be explained by repulsion between EphA4 and EfnB2a-expressing cells. We have therefore proposed that mutual affinity between cells within rhombomeres contributes to boundary formation (Cooke et al., 2005).

We had previously observed that knock-down of EfnB2a strongly enhances the rhombomere boundary phenotype of EphA4 knock-down (Cooke et al., 2005). EfnB2a is expressed in r1, r4 and r7 (Cooke et al., 2005; Xu et al., 1999). We used mosaic analysis to ask whether EfnB2a has a function within these rhombomeres that is analogous to the role EphA4 plays in r3 and r5. We observed that EfnB2a MO cells were excluded from r4 of a WT host embryo where EfnB2a is expressed, but behave normally in other rhombomeres where EfnB2a is not expressed (Fig. 1C); conversely, WT cells formed clusters in r4 of an EfnB2a MO host (Fig. 1D). Similar sorting behaviours were also occasionally observed in r1 and r7 (Figs. 1C, 5C and data not shown). Sorting-out of EfnB2a MO cells was not observed in the midbrain where EfnB2a is also expressed, suggesting that EphA4- and EfnB2a-dependent regulation of cell affinity is a characteristic of the hindbrain neuroepithelium in particular (data not shown). Injection of mRNA encoding full-length EfnB2a rescues the ability of EfnB2a MO cells to contribute to r4 of a WT host (Fig. S1). These results suggest that, like EphA4, EfnB2a promotes cell affinity within the rhombomeres where it is expressed.

We next asked whether the cell sorting we observed in EfnB2a MO mosaic embryos requires EphA4 and vice versa. We found that the sorting-out of EfnB2aMO donor cells from r4 could not be prevented by knocking down EphA4 in host or donor cells; similarly, segregation of WT donor cells into clusters in r3 and r5 of an EphA4 MO host could not be prevented by simultaneously depleting EfnB2a from the host or donor (Table 1 and Fig. 1F). Rhombomere-specific segregation of WT from MO cells was purely additive in all combinations tested. For instance EphA4 MO cells transplanted into an EfnB2a MO host still sort out of r3 and r5 (where EfnB2a is not expressed), just as they would in a WT host; and cluster together in r4 just as WT cells would do in r4 of an EfnB2aMO host (Table 1 and Fig. 1E). Conversely, EfnB2a MO cells transplanted into an EphA4 MO host sort out of r4 and form cell clusters in r3 and r5 (Table 1 and data not shown). Double MO phenotypes were likewise additive: donor cells depleted of both EfnB2a and EphA4 sort out of r3, r4, and r5 in WT hosts (Table 1 and Fig. 1F), whereas transplanting WT cells into EfnB2a; EphA4 double MO hosts leads to clustering in all three rhombomeres (Table 1 and Fig. 5C). These results demonstrate that sorting-out of EphA4 MO cells is not due to up-regulation of EfnB2a and vice versa. Within rhombomeres, EphA4 and EfnB2a do not function as a receptor–ligand pair, but rather independently promote cell affinity within the segments in which they are expressed.

We note that MO donor cells were able to contribute homogeneously and bilaterally to hindbrains of hosts which had been treated with the identical MO combination. For instance, EphA4; EfnB2a double MO donors contributed homogeneously to double MO hosts (Table 1 and Fig. 1G). Thus normal intra-rhombomere cell interactions do not seem to require EphA4 or EfnB2a per se; rather, cells in a given rhombomere can form normal contacts with any neighbours that express an identical Eph or Ephrin "code".

Timing of EphA4- and EfnB2a-dependent cell sorting in mosaics

We have uncovered rhombomere-specific roles in promoting cell affinity for both EphA4 and EfnB2a. We hypothesize that disrupted intercellular adhesion contributes to the severe rhombomere boundary defects we observe in EphA4; EfnB2a double MOs, since the failure of cells with the same rhombomere identity to adhere to one another could result in inappropriate mixing of cells with different rhombomere identities (Cooke et al., 2005). This does not preclude a role for EphA4 and EfnB2a in mutual cell repulsion at boundaries, as has been proposed in previous studies (Xu et al., 1999), since functions for these proteins both within and between rhombomeres would be abolished in the double MO. However, the mosaic embryos in which WT cells segregate from EphA4MO or EfnB2aMO cells provide a way to explore the intra-rhombomere functions of EphA4 and EfnB2a alone. To better understand how differential affinity might impact rhombomere boundaries, we used confocal time-lapse imaging to follow the behaviours of hindbrain cells in mosaic embryos during neurulation.

Genetic mosaics are made by transplanting donor cells into one side of the presumptive hindbrain region of an early gastrula stage embryo (Carmany-Rampey and Moens, 2006). Transplanted cells, which comprise a small minority of the total cells in the neuroepithelium, converge toward the midline with the surrounding host cells, contributing neural progenitors to one side of the forming bilayered neural keel. Starting at ~12 hpf, cross-midline progenitor divisions distribute donor-derived cells to both sides of the keel (Kimmel et al., 1994; Papan and Campos-Ortega, 1999). Cross-midline divisions continue in the neural rod stage up to ~16 hpf, before formation of the neurocoele at ~17 hpf signals the onset of neural tube stage, and a return to planar cell divisions. Previously, we observed that sorting-out of EphA4 MO cells from r3 and r5 of a WT host coincides with the onset of cross-midline cell divisions in the neural keel (Cooke et al., 2005). EphA4 MO donors are never observed to divide across the midline when located in r3 and r5 of a WT host, although they execute normal cross-midline divisions in rhombomeres where EphA4 is not expressed. A similar analysis of WT donor cells forming clusters in EphA4 MO hosts reveals that this cell sorting also coincides with the period of cross-midline cell divisions (Figs. S2, S3). Specifically, donor-derived EphA4+ cells in r3 and r5 at 12.5 hpf are only on the transplanted side of the midline, while donor cells in flanking rhombomeres have begun making cross-midline divisions (Figs. 2A, B). Clumps in r3 and r5 are readily identified at 14.5 hpf, becoming tight, well-formed unilateral WT cell clusters by 18 hpf (Figs. 2C, D). In contrast, bilateral WT donor-derived cells are present in non-EphA4-expressing rhombomeres at the neural tube stage (Fig. 2D). To determine whether EfnB2a-based cell sorting in the hindbrain occurs with similar timing, we performed confocal timelapse imaging of EfnB2a MO cell sorting from r4 of WT embryos (Fig. S4). Initially, donor cells at the neural plate stage were evenly distributed along the anterior–posterior axis on the transplanted side of the hindbrain. At the onset of the neural keel stage, donor EfnB2a MO cells were observed making midline-crossing cell divisions in r2, r3, r5 and r6, but not r1 or r4 (Fig. S4). By the end of the timelapse, at the neural tube stage, donor-derived bilateral clones were apparent in r2, 3, 5 and 6, whereas EfnB2a MO cells were only observed on the transplanted side

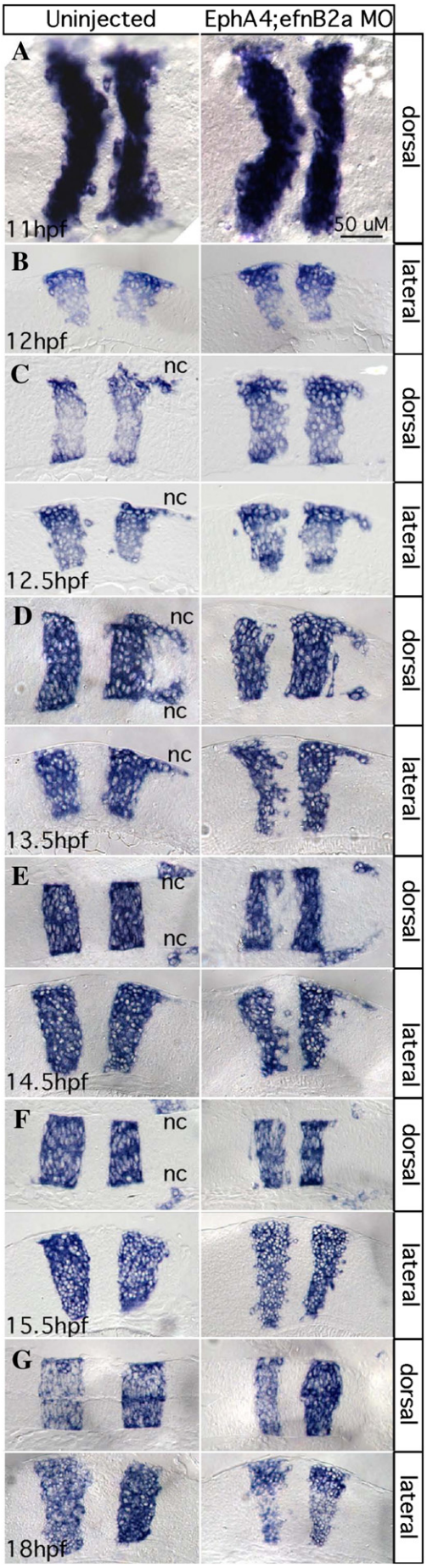

of r1 and r4 (Fig. S4). As we observed previously in EphA4MO mosaics, EfnB2a MO cells initiate cross-midline divisions at the edges of EfnB2a-expressing rhombomeres when they contact EfnB2a-negative cells in the adjacent rhombomeres (Figs. 1C, F). From this analysis we conclude that EfnB2a-based cell sorting in the hindbrain occurs with similar timing and affects the same cellular behaviours as the sorting observed in EphA4 MO genetic mosaics.

Timing of rhombomere boundary defects in EphA4MO; EfnB2aMO embryos

Based on time-lapse analysis of mosaic embryos described above we conclude that the requirement for EphA4 or EfnB2a within rhombomeres begins at the onset of cross-midline divisions, as the keel is forming at ~12 hpf. We imaged forming rhombomere boundaries at high temporal and spatial resolution in fixed WT and EphA4; EfnB2a double MO embryos by RNA in situ hybridization using *krox20*/*egr2b*. We observed that the organization of cells at forming rhombomere boundaries was identical in the WT and EphA4;EfnB2a double MO before the neural plate-to-neural keel transition at ~12 hpf (Figs. 3A, B). From 12.5 hpf on, boundaries were already quite sharp in the WT, whereas double MO boundaries became more disorganized at 12.5 hpf and were strongly disorganized at 13.5 hpf (Figs. 3C, D). At 13.5 hpf and 14.5 hpf, many cells exhibiting r3 or r5 identity (*krox20*+) were observed encroaching into r4 territory (Figs. 3D, E). From this we conclude that boundary sharpening is initially normal in the absence of EphA4 and EfnB2a, but then decays after 12 hpf. The timing of boundary decay therefore corresponds with the timing of EphA4- and EfnB2a-dependent sorting observed in mosaic embryos. We observed that in many double MO embryos, starting as early as 12 hpf, rhombomere morphology was abnormally tall and thin, in spite of normal hindbrain width indicative of normal convergent extension movements. This phenotype became more dramatic at later time-points. One possibility is that when dividing cells in the keel are no longer constrained to one rhombomere, the resulting chaotic intercalation of cells from different rhombomeres drives an overall dysmorphogenesis of the hindbrain. At later stages, loss of Notch signaling from rhombomere boundaries could result in a reduction in the number of cells and rhombomere thinning (Cheng et al., 2004).

At later neural rod stages (15.5 hpf), the disorganized boundary phenotype became less severe in the double MO, but overall rhombomere morphology remained abnormal (Fig. 3F). At the neural tube stage (18 hpf), r3 and r5 were unequal and asymmetrical in the double MO as compared to the uninjected control (Fig. 3G).

Mis-localized neural rod cells exhibit plasticity independently of EphA4

We noted that the boundaries of *krox20*/*egr2b* expression in EphA4; efnB2aMO embryos became sharper after the end of the neural keel stage (Fig. 3). This could be due to residual Eph–Ephrin dependent cell sorting in these knock-down embryos, or to other mechanisms that can sharpen boundaries of gene expression. By transplanting cells singly or in small groups between rhombomeres at the neural rod stage, we observed that individual cells can exhibit plasticity, changing their identity from that of their rhombomere of origin (Figs. S5A, B), consistent with previous studies showing plasticity of cells transplanted between hindbrain segments (Itasaki et al., 1996; Schilling

Fig. 3. EphA4 and EfnB2a mediate hindbrain boundary sharpening during the neural keel stage. Whole mount (A) and 10 μm plastic sections (B–G) of RNA in situ hybridizations with a *krox20*/*egr2b* riboprobe. Anterior is to the left, dorsal or lateral views are indicated. Left panels show uninjected control embryos; right panels show stage-matched EphA4; EfnB2a double MO embryos. (A) Neural plate stage (N=20); (B) neural plate to neural keel transition; (C, D) successive neural keel stages; (E, F) successive neural rod stages; (G) neural tube stage. Nc: r5-derived neural crest. Representative sections for each timepoint were chosen from at least 8 identically treated embryos. Scale bar: 50 μm.

et al., 2001). We observed that the ability of cells to change their identity was independent of EphA4: approximately 80% of donor cells transplanted from r3 to r4 at the 10–12 s stage lose *krox20/egr2b* expression regardless of whether they express EphA4 or not (Fig. S5C). We hypothesize that this EphA4-independent plasticity may contribute to the sharpening of *krox20* expression boundaries in later EphA4; efnB2a double MO embryos. However we note that in spite of this activity, rhombomere boundaries remain disrupted with significant consequences for hindbrain neuroanatomy (Cooke et al. 2005).

Bilateral EphA4 expression is required for cross-midline divisions

The above observations focused our attention on the role of EphA4 and EfnB2a during the period of mirror-symmetric progenitor cell divisions, which begins ~12 hpf. We hypothesize that the inability of donor cells to generate bilateral clones in rhombomeres occupied by host cells expressing a different Eph or Ephrin "code" is due to a failure to complete cross-midline cell divisions. Careful analysis of time-lapses of WT to EphA4 MO mosaics revealed that the failure of donor cells to generate bilateral clones in r3 and r5 is not due to the inability of donor cells to divide (Fig. S6). During the neural keel stage (12–16 hpf), WT donor cells in an EphA4 MO host r3 or r5 segment do divide with the same timing as donor cells in r4 (Figs. 4A–F). However, whereas WT donor cells in r4 successfully contribute daughters to both sides of the neural keel, donor-derived daughter cells in r3 and r5 remain on the same side of the midline and form unilateral clusters.

We considered a number of possible reasons for the failure of WT neural progenitors to cross the midline in EphA4 MO hosts. During

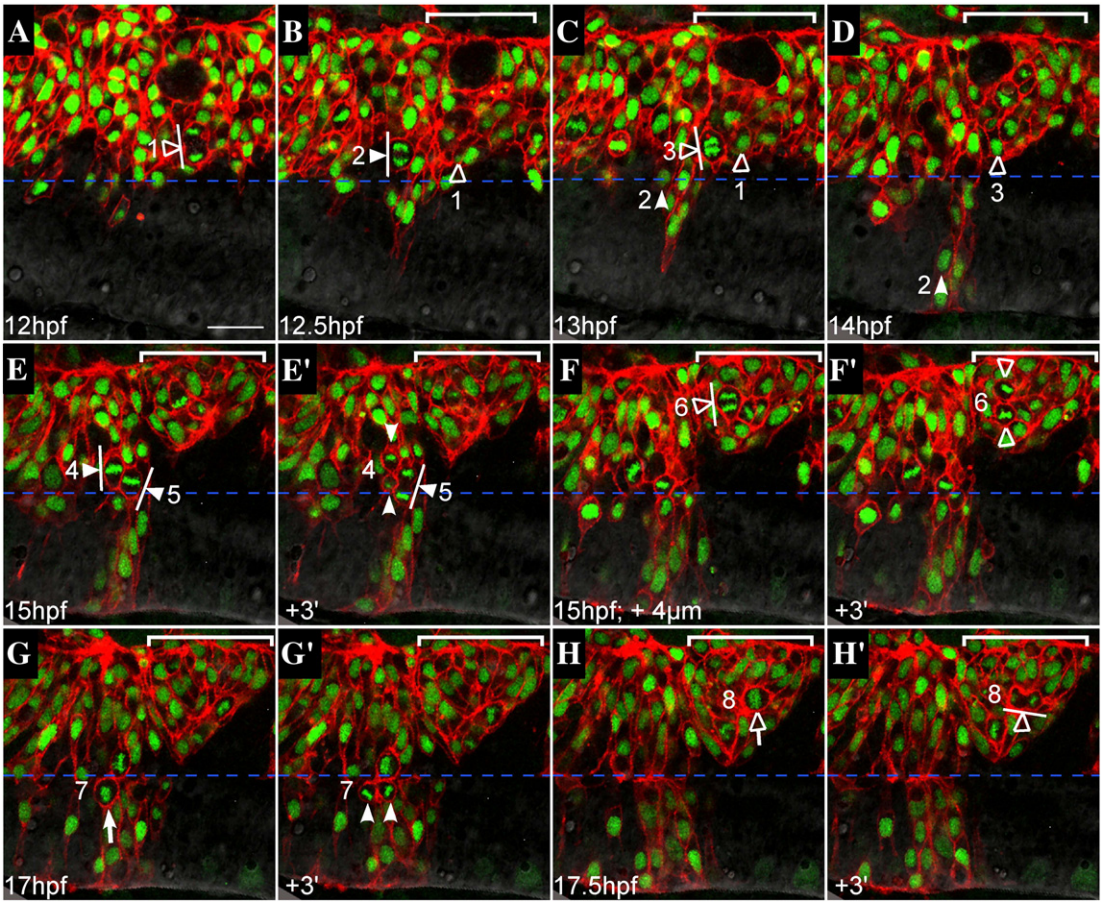

Fig. 4. Failure to generate bilateral clones is not due to a defect in oriented cell divisions. Representative confocal sections from a time-lapse of a mosaic embryo, dorsal views, anterior to the left. WT donor cells (expressing mRFP to visualize cell membranes, histone-GFP to visualize nuclei) were transplanted into an EphA4MO pGFP5.3 host embryo (expressing GFP in r3 and r5; not shown). Midline is indicated by horizontal dashed blue line. r5 is indicated by white bracket in upper right hand corner of most images. Cells entering mitosis (rounded up; condensed chromatin) are indicated by white (r4) or hollow (r5) arrows. Cells in mitosis are indicated by arrowheads ending in perpendicular lines that represent spindle orientation. Daughters of numbered divisions that are still in the plane of focus are indicated by arrowheads. (A) At the onset of neural keel stage (12 hpf), donor cells are evenly distributed up to the midline throughout the hindbrain. Because the transgene is not expressed in r5 at this early timepoint, r4 and r5 territories cannot be definitively assigned. However a cell that is unambiguously assigned in later timepoints to r5 has already entered anaphase and is positioned close to the midline (hollow arrowhead; division "1"). (B) At early neural keel (12.5 hpf), a WT donor cell in r4 divides with a medial nuclear position and transverse spindle orientation (white arrowhead; division "2"). The more medial daughter from division "1" is located in r5. (C) At 13 hpf a donor cell in r5 divides medially with transverse spindle orientation (hollow arrowhead; division "3"). Meanwhile, the more medial daughter of division "2" has begun to cross the midline (white arrowhead). The other daughter from division "2" remains on the transplanted side of the neuroepithelium throughout the timelapse (different plane of focus; data not shown). (D) By 14 hpf, one daughter from division "2" (white arrowhead) has completed midline crossing and is integrated into the contralateral side of the neuroepithelium, whereas the more medial daughter from division "3" (hollow arrowhead) remains on the original side of the neuroepithelium. Both daughters of division "3" were tracked for an additional 2 h and failed to cross the midline during this time (data not shown). (E) At 15 hpf, two WT donor cells in r4 with medially positioned nuclei are in metaphase with mitotic spindles orientated transverse to the midline (white arrowheads; divisions "4" and "5"). (E′) Within 3 min, a dividing cell from panel C has entered telophase (white arrowhead; division "5") and another has completed cytokinesis, generating a more medial and more lateral daughter cell (white arrowheads; division "4"). (F) At the same timepoint as in panel E (15 hpf), but 4 µm deeper into the embryo, a laterally displaced WT donor cell in r5 (hollow arrowhead; division "6") is shown at anaphase with a transverse spindle orientation (white line). (F′) Within 3 min, the dividing cell from panel F has completed cytokinesis, generating a more lateral and a more medial daughter cell (hollow arrowheads), neither of which crosses the midline during the course of the timelapse (data not shown). (G) WT donor cell in r4 at the neural tube stage (17 hpf) rounds up prior to division with medial nuclear position (white arrow; division "7"). (G′) Donor cell indicated in panel G has completed cytokinesis. Daughters of this division are born side by side, equidistant from the midline (white arrowheads). (H) Laterally displaced WT donor cell in r5 rounds up and has condensed chromatin prior to mitosis (hollow arrow; division "8"). (H′) Within 3 min, the dividing donor cell from panel H has entered telophase. Spindle orientation is planar, ie. parallel to the midline (white line). Scale bar: 25 µm.

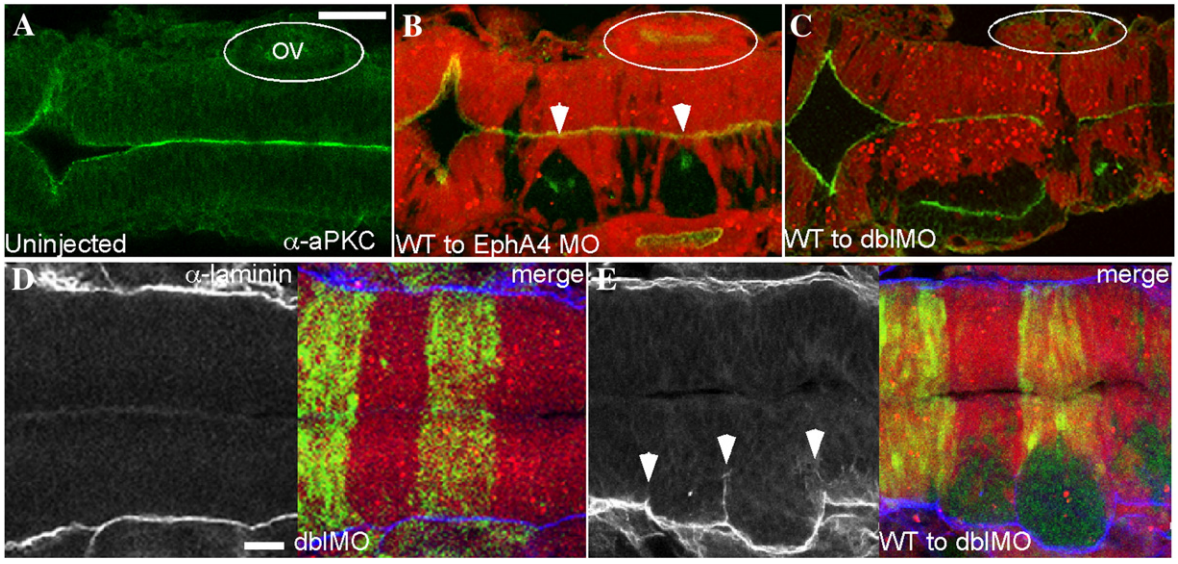

Fig. 5. Failure to execute cross-midline divisions results in duplicated neuraxes in EphA4 and EfnB2a MO mosaics. Immunostaining of 18 hpf mosaic embryos shown in dorsal view with anterior to the left. (A–C) merged images showing α-aPKC (green) and MO host cells labelled with rhodamine (red). (A) aPKC is expressed on the apical surface of neuroepithelial cells, which is at the midline. (B) WT EphA4+ donor cells (unlabelled) fail to cross the midline and form unilateral clusters in r3 and r5 when transplanted into an EphA4MO host (white arrowheads); these clusters have an ectopic aPKC+ apical region. Likewise WT EfnB2a+ donor cells form a unilateral cluster in r4 of an EfnB2a MO host (data not shown). (C) WT cells transplanted into an EphA4; EfnB2a double MO host form three separate clumps with ectopic apical surfaces (data not shown) or fuse to give rise to a partially duplicated neuroepithelium in the r3–r5 region; cell clustering is also sometimes evident in r7 (N=6). OV (otic vesicle). (D,E) α-laminin staining (left panels); right panel is a merge showing the rhodamine-labeled double MO host cells (red); host cells contain the pGFP5.3 transgene and express GFP in r3 and r5 (green). (D) Laminin is expressed along the lateral edges of the neuroepithelium in WT (not shown) and in double MO host embryos (N=24). (E) Laminin is ectopically expressed around the edges of the cluster of unlabelled WT cells in a WT to double MO mosaic embryo (N=27). Scale bars: 50 μm.

cross-midline divisions in the neural keel, cells re-orient their spindles to allow division in an apico-basal direction as compared to the planar divisions that occur earlier in the neural plate stage and later in the neural tube (Geldmacher-Voss et al., 2003; Tawk et al., 2007). Improper spindle orientation could thus lead to the failure of donor-derived cells to cross the midline. In our time-lapse analysis, cells throughout the hindbrain were observed to undergo planar cell divisions during the neural plate stage (data not shown) and also later in the neural tube (Figs. 4G, H). From 12.5 hpf to 16 hpf (neural keel/rod) in r4, spindle orientation at anaphase was apico-basal in 100% of cell divisions and in 71% of these, the medial-most daughter was observed crossing the midline (Figs. 4B, D, E and Table 2). 75% of donor cell divisions in r3 and r5 were similarly apico-basal in orientation, even though none of these divisions resulted in bilateral daughters (Figs. 4C, D, F and Table 2). Thus spindle orientation alone is insufficient to explain the failure of these cells to cross the midline in mosaic embryos.

As in other epithelia, both planar and apico-basal divisions in the developing neuroepithelium occur with the nucleus positioned close to the apical surface, which in the neural keel stage zebrafish embryo is the midline. We noted that while donor cell divisions in r4 of an EphA4MO host occurred at the midline, many cell divisions in r3 and r5 occurred laterally, away from the midline (Figs. 4E, F and Fig. S6). Systematic scoring of the mediolateral position of dividing nuclei revealed that in r4, 92% of labeled WT cells divided in the most medial section of the neural keel/rod whereas in r3 and r5, over 80% of WT cells were positioned abnormally laterally (Table 2). Therefore it is possible that the more lateral position of dividing donor cells in r3 and r5 contributes to their failure to cross the midline. We note that the lateral position of these divisions is not due to a failure of cells in r3

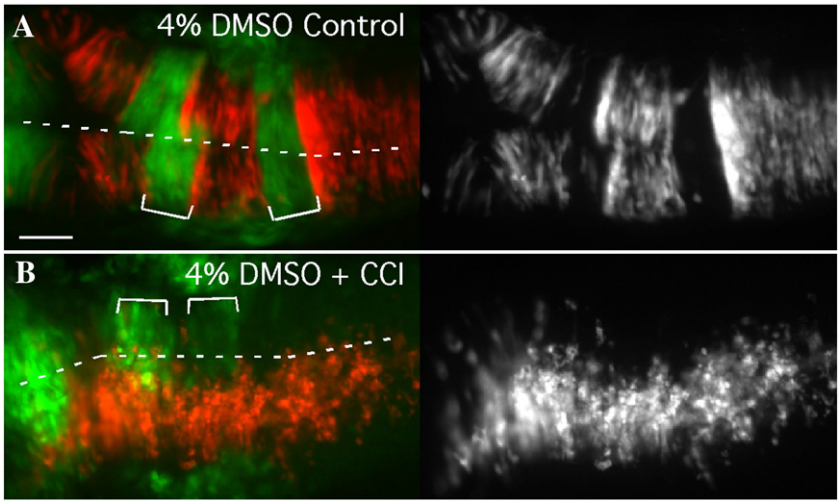

Fig. 6. Cell sorting is prevented by inhibiting cell division in the neural keel/rod. Dorsal views of 18 hpf mosaic embryos with anterior to the left. (A) EphA4 MO donor cells (red) sort out of r3 and r5 of a WT pGFP5.3 host (green) treated with solvent alone (4% DMSO; *N*=10). (B) Treatment of mosaic embryos from 90% epiboly onwards with cell cycle inhibiting drugs inhibits cross-midline divisions and also prevents sorting-out of EphA4MO cells from r3 and r5 (*N*=7/11). Scale bar: 50 μm.

and r5 to converge to the midline, because at the onset of the neural keel stage, it is not possible to distinguish donor-derived cells in r3 and r5 from donor-derived cells in other rhombomeres based on their mediolateral position (Fig. 4A). Rather, there is a progressive lateral displacement of the donor cells away from the midline in r3 and r5, suggesting a failure to maintain normal contact with contralateral progenitors whose EphA4 levels are different (Figs. 4A–F and Fig. S7).

Tawk et al., (2007) observed that when neuroepithelial cells attempt mirror-symmetric divisions at positions displaced from the midline of the forming neural keel, this can result in a duplicated neuraxis with its own apico-basal polarity (Tawk et al., 2007). Consistent with this, we observed that donor-derived WT cell clusters in EphA4MO mosaics and EfnB2aMO mosaics form incipient duplicate neuraxes, with an ectopic "midline", marked by aPKC or Pard3 protein adjacent or perpendicular to the host midline (Fig. 5B and data not shown). Furthermore, when WT cells are transplanted into hosts lacking both EfnB2a and EphA4, the cell clusters they form in r3, r4 and r5 sometimes fuse to create a duplicated hindbrain neuraxis in that region (Fig. 5C). Laminin expression at the edges of the WT cell clusters reveals that the clusters of WT cells contain a corresponding ectopic basal surface (Figs. 5D, E). Neurogenesis takes place at the lateral edge of the neuroepithelium in WT (not shown) and double MO (Fig. S8A) embryos, as well as the ectopic basal surface present in WT cell clusters (Fig. S8B). Duplication of the Mauthner neuron is occasionally observed in the duplicated hindbrain region (Fig. S8C–E). Together, these results suggest that EphA4 and EfnB2a regulate cell intercalation during the cross-midline cell divisions that characterize the neural keel/rod stage of neural development.

EphA4-dependent cell sorting can be rescued by preventing cross-midline cell division

In mosaic embryos, we observe that unilaterally transplanted donor cells fail to divide across the midline in spite of normal cell polarity and spindle orientation. Because donor cells exhibit this defect only in rhombomeres where they are surrounded by cells that have different EphA4 or EfnB2a levels, we hypothesize that this cross-midline division defect is secondary to a failure to establish normal contacts with contralateral neighbours that have a different Eph–Ephrin "code". We specifically suggest that the subsequent sorting movements of donor cells are driven by the successful cross-midline divisions of surrounding host cells. If this is true, we reasoned that by blocking the cell cycle during cross-midline divisions in mosaics we could rescue this phenotype. Indeed, treatment with cell cycle inhibitors during neural keel/rod stage prevents the sorting out of EphA4 MO cells in a WT host (Fig. 6). Under these conditions, all donor-derived cells are unilateral because they are prevented from executing the cross-midline division; however they also do not sort out of r3 and r5, presumably because contralateral wild-type cells are prevented from dividing across the midline and pushing the less cohesive MO donor cells aside. We note, however, that this experimental paradigm does not rule out the possibility that cell division and intercalation between cells on the same side of the neural keel also contributes to cell sorting movements. Indeed, EphA4 and EfnB2a are expressed all around the cell periphery, not just at the midline, and therefore are likely to regulate ipsilateral cell interactions.

EphA4 or EfnB2a over-expression inhibits cross-midline cell division

We reasoned that if neural progenitors undergoing cross-midline cell divisions can only form normal contacts with cells expressing the same Eph or Efn on their cell surface, then even differences in the levels of these proteins might drive cell sorting. We asked whether mosaic over-expression of either EphA4 or EfnB2a prevented dividing cells from crossing the midline. Previously, Xu et al. showed that mosaic over-expression of EphA4 mRNA in zebrafish embryos caused cells to be excluded from EfnB2a-expressing rhombomeres and vice versa, consistent with EphA4–EfnB2a-mediated repulsion (Xu et al., 1999). In the course of performing mRNA rescue experiments for our MO phenotypes we confirmed these observations: EphA4 mRNA concentrations that rescue the ability of EphA4 MO cells to contribute to r3 and r5 of a WT host embryo cause exclusion of donor cells from EfnB2a-expressing r4 (Cooke et al., 2005), and EfnB2a mRNA levels that rescue the ability of EfnB2a MO cells to contribute to r4 simultaneously inhibit donor cells from crossing the midline into EphA4-expressing r3 and r5 (Fig. S1C). However we also observed that WT donor cells expressing the same "rescuing" amount of ectopic EphA4 are additionally excluded from the contralateral side of r3 and r5 (data not shown), and WT cells expressing the "rescuing" amount of exogenous EfnB2a similarly form unilateral clusters in r4 (Fig. S1D). In these contexts the donor-derived cells are over-expressing EphA4 or EfnB2a because they express the protein from both the endogenous locus as well as the exogenously supplied mRNA; in contrast, the WT host cells express only the endogenous gene. This was confirmed by Western blot analysis (data not shown). Interestingly, overexpression of an EfnB2aΔC-GFP allele in which the C-terminus of EfnB2a is replaced with GFP still mediates segregation of donor cells from cells in WT r4 (Fig. S1E). We observe segregation even when over-expressing cells are coinjected with EfnB2a MO (Fig. S1F). Furthermore, we note that the sorting phenotype resembles the phenotype of clustering observed in WT to MO embryos, suggesting that donors have increased cell affinity rather than reduced cell affinity, in which case we would expect to see donors being sorted to the r4 boundaries, just as happens in MO to WT mosaics. Based on these observations, we do not believe that the truncated allele exerts its effects on sorting by acting as a dominant negative. It is therefore possible that EfnB2a-based adhesion does not require reverse signaling. The inability of the donor cells which over-express EphA4 or EfnB2a to cross the midline in rhombomeres populated by host cells that express WT levels of the very same Eph or Ephrin suggests that different levels of EphA4 or EfnB2a on the cell surface are sufficient to drive cell sorting. These results support our hypothesis that neural progenitors can only integrate normally into hindbrain segments that express the identical suite of Ephs and Ephrins, at equivalent levels.

A concern about the over-expression experiments described above is that ectopic expression of EphA4 or EfnB2a during gastrulation could delay convergent extension movements of the neuroepithelial progenitors and result indirectly in their failure to generate bilateral clones (Tawk et al., 2007). We injected a heatshock-inducible construct to drive mosaic co-expression of EfnB2a and GFP after the end of gastrulation. Unlike in transplantation mosaics, heat shock induces EfnB2a expression mosaically on both sides of the neuroepithelium; nonetheless, successful cross-midline divisions are still expected to generate bilateral GFP+ clones. Heat-shock induction of GFP alone, or injection of the EfnB2a expression constructs without heat-shock did not cause hindbrain defects (Fig. 7A and data not shown). In contrast, induction of EfnB2a expression immediately before or at the normal onset of cross-midline divisions (by heat shock at 10 hpf or 12 hpf) results in a dramatically disorganized hindbrain with many GFP+ cells that lack a mirror-symmetric daughter, which we interpret as failure of these ectopically expressing cells to complete the cross-midline division (Fig. 7B). Staining with α-EfnB2a confirmed that GFP+ cells co-express high levels of EfnB2a (data not shown). Mosaic induction of EfnB2a by heat shock at 10 hpf or 12 hpf also frequently induced partial neuraxis duplication as revealed by aPKC immunostaining (Fig. 7C). Duplication of the hindbrain neuroepithelium was more complete when embryos were simultaneously depleted of endogenous EfnB2a (Fig. 7D). Consistent with results obtained from mRNA over-expression mosaics using the EfnB2aΔC-GFP allele (Fig. S1E), mosaic expression at 10 hpf or 12 hpf of a truncated form of EfnB2a that lacks the intracellular domain (EfnB2a-ΔC) also inhibits formation of bilateral

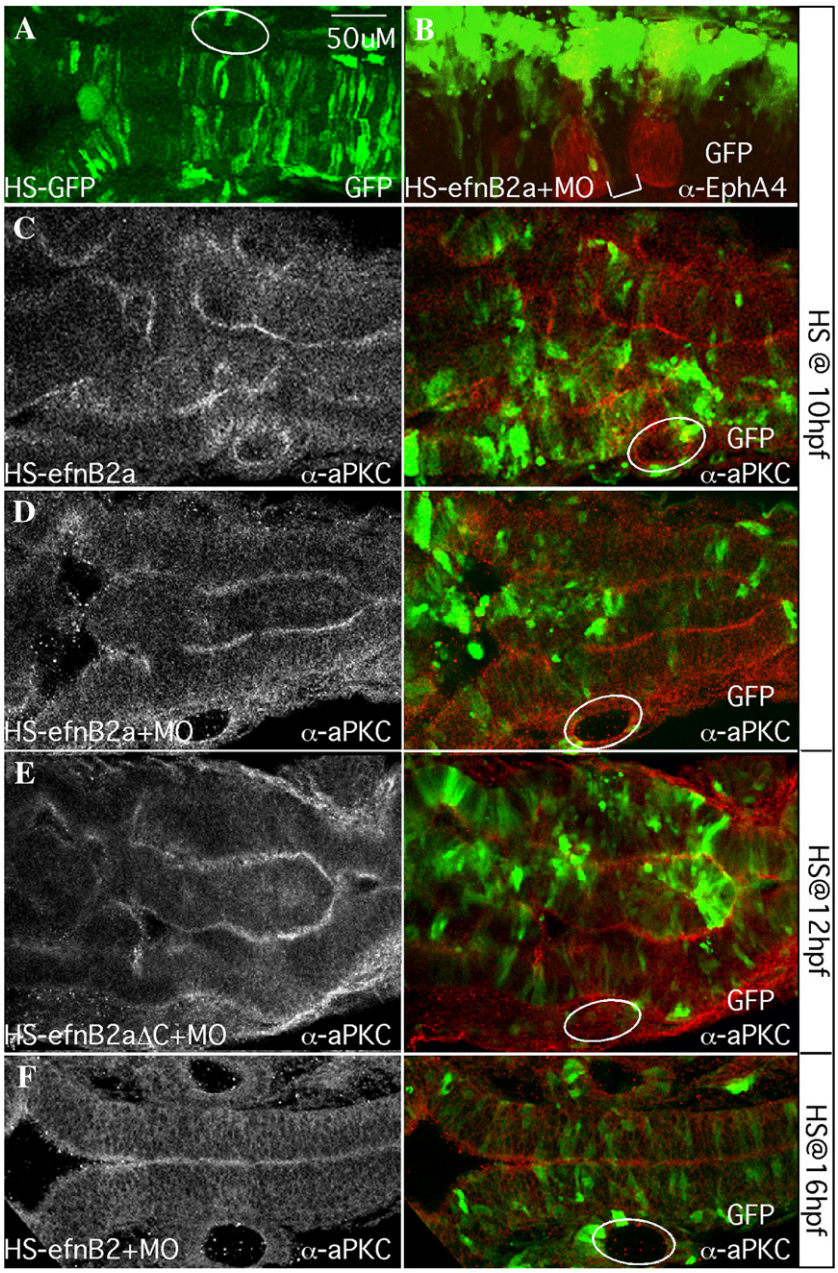

Fig. 7. Mosaic EfnB2a overexpression in the neural keel causes widespread cell sorting and duplication of the neuraxis. Dorsal views of 18–20 hpf embryos injected with heat-shock (HS)-GFP (A) or HS-EfnB2a DNA constructs (B–F) as indicated. Anterior is to the left. White circles indicate the position of the otic vesicle. (A) pHS-GFP-injected embryo coinjected with EfnB2a MO, and heat shocked at 10 hpf. GFP+ cells are symmetrically distributed on both sides of the neuroepithelium (N=12/12). (B) pHS-EfnB2a-HS-GFP injected embryo coinjected with EfnB2a MO, heat shocked at 10 hpf and stained with α-EphA4 to detect r3, r5 (red). r4 is indicated with a white bracket. EfnB2a+/GFP+ cells (green) are distributed asymmetrically throughout the hindbrain, including in r4 (N=16/27). (C–F) Embryos injected with the indicated HS constructs, with or without EfnB2a MO, heat shocked at the timepoint indicated on the far right and stained with α-aPKC. Left panel: aPKC expression alone; right panel: merged image showing distribution of EfnB2a+/GFP+ cells (green) and aPKC expression (red). (C, D) Embryo injected with pHS-EfnB2a-HS-GFP in the absence or presence of coinjected EfnB2a MO, heat shocked at 10 hpf. aPKC expression in two parallel stripes reveals partial duplication of the neuraxis (N=7/14, and 9/14, respectively). (E) Embryo injected with the HS-EfnB2a-ΔC allele and EfnB2a MO, heat shocked at 12 hpf also shows neuraxis duplication (N=9/20). A similar phenotype is observed when embryos are injected with the WT EfnB2a allele HS construct, in the absence or presence of EfnB2a MO, and heat shocked at 12 hpf (data not shown; N=3/7, and 5/8, respectively). (F) Embryo co-injected with pHS-EFnB2a-HS-GFP and EfnB2a MO, then heat shocked at 16 hpf. EfnB2a-expressing cells contribute homogeneously to the epithelium and no duplication of the neuroepithelium has occurred (N=14/14). Immuno-staining confirms that EfnB2a expression is still ectopically induced in embryos heat shocked at 16 hpf (data not shown; N=7/7). Scale bar: 50 μm.

clones and causes disorganization and duplication of the neuroepithelium, in the presence or absence of endogenous EfnB2a (data not shown and Fig. 7E). In fact, the phenotype is more severe when endogenous EfnB2a is depleted by coinjection with MO, suggesting that the sorting activity driven by this allele is not a dominant negative effect and the intra-rhombomere function for EfnB2a does not require canonical reverse signaling. Importantly, induction of EfnB2a expression at 16 hpf, after cross-midline divisions are complete, results in a normal hindbrain neuroepithelium with EfnB2a-expressing cells distributed evenly throughout the hindbrain, including in Eph-expressing rhombomeres (Fig. 7F). We conclude that normal cross-midline divisions in the hindbrain require equivalent bilateral levels of EphA4 and EfnB2a.

Discussion

We have previously shown that loss of EphA4, a receptor tyrosine kinase expressed in r3 and r5 of the developing hindbrain, causes a

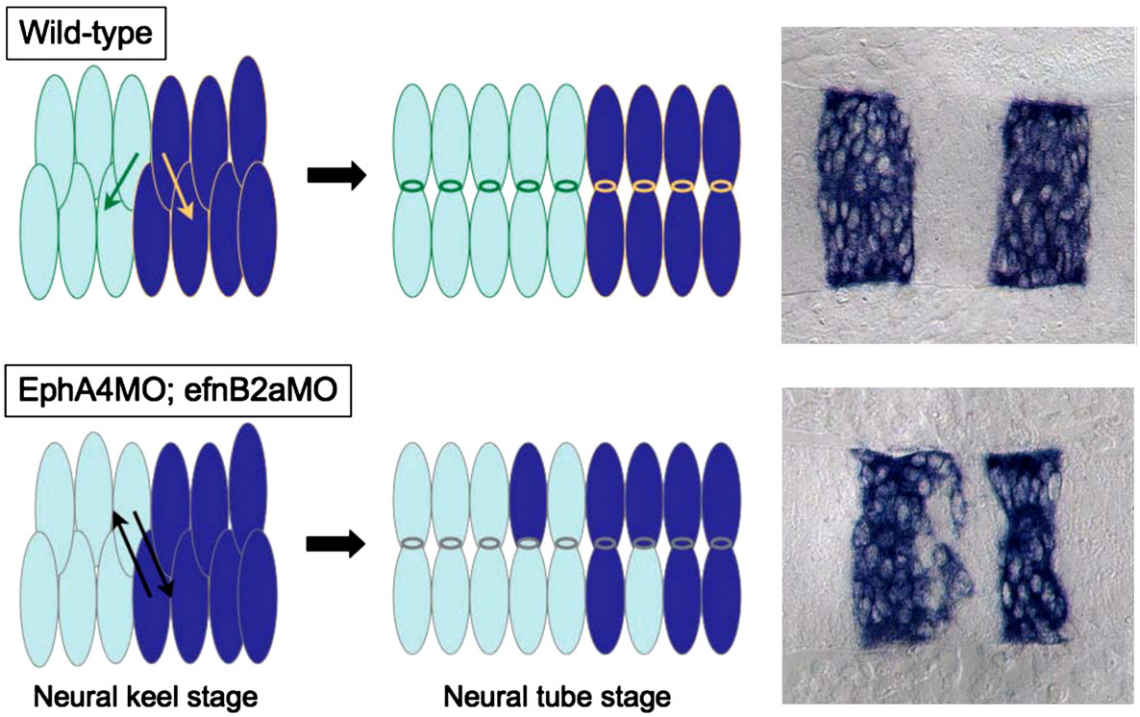

Fig. 8. A model: unrestricted cross-midline divisions disrupt rhombomere boundaries in an EphA4; EfnB2a MO embryo. In a WT hindbrain, daughter cells created by cross-midline divisions in r3, r4 and r5 are restricted by the presence of cell surface EphA4 and EfnB2a to intercalate well inside their respective rhombomeres of origin. Neuroepithelial cells in r3–5 in embryos lacking EphA4 and EfnB2a divide without such restrictions, leading to mis-sorting of daughters from r3 and r5 mothers into r4 and vice versa.

hindbrain boundary defect, a phenotype exacerbated by simultaneous loss of its ligand, EfnB2a, which is expressed in the intervening r4 segment. Based on genetic mosaic analysis which revealed that EphA4+ cells in r3 and r5 sort out from EphA4 MO cells in the same territory, we previously proposed a model in which adhesion between EphA4+ cells within r3 and r5 contributes to robust rhombomere boundary formation. Here we show that EfnB2a mediates cell affinity within r4. Indeed, our experiments demonstrate that EphA4 and EfnB2a, which in other contexts act as a canonical receptor–ligand pair, function independently of one another within their respective hindbrain territories. Our data further suggests that normal function of these molecules in the zebrafish hindbrain is critical during the cross-midline cell divisions that begin as the neural keel is forming at 12 hpf and which drive the dramatic extension of the neuraxis during this period of development. Specifically, the boundary defect in EphA4; EfnB2a double MO is first observed at the same stage as EphA4MO or EfnB2a MO cells begin to sort away from WT rhombomeres in mosaics, and both phenomena coincide with cross-midline cell divisions in the neural keel/rod stage of teleost neurulation. In either loss- or gain-of-function mosaics, cells that have different EphA4 or EfnB2a levels from their contralateral neighbours in the hindbrain at the neural keel/rod stage fail to divide across the midline, resulting in widespread disorganization of the hindbrain; however, misregulation of EfnB2a levels after the completion of cross-midline cell divisions has no phenotype. We hypothesize that the misplaced cells in double MO embryos could have arisen in the course of unconstrained cross-midline divisions. We therefore propose a model in which the segmental regulation of cell affinity by EphA4 and EfnB2a ensures that progenitor cells intercalate between cells with the same rhombomere identity during cross-midline divisions, thereby maintaining rhombomere boundaries by preventing cells from one rhombomere territory from dividing into adjacent rhombomeres (Fig. 8). Our data does not rule out possibility that an EphA4–EfnB2a interaction at rhombomere boundaries is required for rhombomere boundary integrity. We also acknowledge that EphA4 and EfnB2a localize all around the cell periphery, not just at the midline and therefore likely mediates ipsilateral inter-cellular interactions.

EphA4 and EfnB2a regulation of cell adhesion during mitosis affects hindbrain morphology

Our work suggests that EphA4 and EfnB2a function during the apico-basal divisions of neuroepithelial progenitors in the neural keel/rod. Strictly timed and oriented cell divisions underlie many developmental events, including differentiation and morphogenesis. In neuroepithelia, oriented asymmetric division is considered to be an important factor in differentiation. For instance, apico-basal divisions in the mammalian cortex are thought to be neurogenic (Chenn and McConnell, 1995; Reid et al., 1997). Although vertebrate Ephs and Ephrins have not previously been shown to function during oriented cell divisions, a role for EfnA has recently been described in an asymmetric cell division leading to differentiation in *Ciona* (Picco et al., 2007). In the teleost neural keel/rod, apico-basal divisions are symmetric, giving rise to bilateral neural progenitors (Geldmacher-Voss et al., 2003; Tawk et al., 2007); in this context Eph and Ephrin control morphogenesis rather than differentiation. We observe that cells with different EphA4 levels than their contralateral neighbours frequently divide at positions away from the midline, suggesting a failure to establish normal adhesive interactions across the midline during the infolding of the neural keel. It has been shown that the orientation of cell divisions in the neural keel defines the apico-basal axis of the resulting daughters (Tawk et al., 2007), so that lateral displacement of progenitors resulting from delayed convergent-extension movements gives rise to neural tube duplication. In our EphA4 MO mosaics, differential cell affinity leads to the generation of ectopic "midlines" in clusters of donor-derived cells. This suggests that the same morphogenetic phenotype can be generated by any mechanism that laterally mispositions neuroepithelial progenitors in the neural keel. We hypothesize that disruption of any mechanism affecting cell affinity in the hindbrain would have the same phenotype as we have observed.

Eph and Ephrin signaling in the hindbrain

The Eph–Efn interaction has the unusual ability to initiate signaling in both the receptor-expressing ("forward signaling") and ligand-expressing ("reverse signaling") cells. The EfnB intracellular domain includes several conserved signaling motifs that have been shown to mediate reverse signaling (Bong et al., 2004; Cowan and Henkemeyer, 2001; Lu et al., 2001; Makinen et al., 2005; Palmer et al., 2002; Torres et al., 1998). In our assays, EfnB2a alleles lacking the intracellular domain behaved similarly to WT EfnB2a, even in the absence of endogenous EfnB2a, suggesting that the intra-rhombomere function for EfnB2a does not require reverse signaling. Although EfnBs homodimerize, leaving open the possibility that the truncated allele has a dominant negative effect on EfnB2a function, we do not believe that to be the case in our experiments. First, the phenotype of cells expressing the truncated allele is not that they are sorted to the r4 boundary, as happens in MO to WT mosaics and which would be consistent with an overall reduction in EfnB2a function. Rather, these donors cluster together and fail to cross the midline, consistent with increased cell affinity, just as is seen in WT to MO mosaics or when cells over-express WT EfnB2a. Second, over-expression of the truncated allele still mediates cell sorting even if donors are coinjected with EfnB2a MO, suggesting that the truncated protein does not need to bind the WT EfnB2a protein in order to exert its effects on sorting. The ability of EfnB2a to affect cell sorting in the absence of its cytoplasmic domain is reminiscent of a previous study which concluded from EfnB2a over-expression experiments that unidirectional signaling is sufficient to drive cell repulsion in the hindbrain (Xu et al., 1999). Given that we observe robust sorting-out of EfnB2a-overexpressing cells even from rhombomeres where EphA4 is not expressed, it seems possible that the sorting of EfnB2a-expressing cells observed in the earlier work was driven at least in part by cohesion of EfnB2a-expressing cells, rather than solely by mutual repulsion between EfnB2a- and EphA4-expressing cells.

It remains to be determined what molecules lie up and downstream of EphA4 and EfnB2a to regulate cell affinity within rhombomeres. While other receptors and ligands are expressed in the hindbrain – notably, EfnB3 is expressed in r2, 4, and 6, while EphB4a is expressed in r2,3,5,6 (Cooke et al., 2001, 2005) – no Ephrin ligands for EphA4 have been shown to be specifically expressed in r3 and r5, nor have Eph receptors for EfnB2a been shown to be expressed specifically in r4. However the expression patterns of zebrafish Ephs and Efns have not been fully described and we cannot rule out the possibility that low level, non-rhombomere restricted expression of ligands or receptors in the hindbrain underlie the rhombomere-specific functions for EphA4 and EfnB2a. The effects on differential cell affinity suggest that EphA4 and EfnB2a signaling results in changes to cell adhesion machinery, possibly by affecting the levels or localization of adhesive proteins like cadherins or integrins. Previous studies both in vivo and in vitro have demonstrated a connection between Eph–Efn signaling and adhesion. Eph–Ephrin interactions can be intrinsically adhesive if they are not actively cleaved or internalized (Janes et al., 2005; Marston et al., 2003; Zimmer et al., 2003). Indeed, adhesion between EphA7 and EphrinA5, which are co-expressed in the mammalian neural folds, is required for neural tube closure in the mammalian forebrain (Holmberg et al., 2000). While teleost neural keel formation and mammalian neural tube closure are developmentally distinct events, both involve the apical adhesion of neural progenitors from the left and right sides of the embryo, and defects in either process result in severe neural tube defects (Ciruna et al., 2006; Tawk et al., 2007; Wallingford, 2005). It is interesting that the two processes may also be mechanistically similar in their requirement for Eph–Ephrin signaling.

An alternative possibility is that EphA4- and/or EfnB2a-dependent cell interactions in the hindbrain do not require binding to canonical partners. On the basis of affinity data, it had already been proposed that Ephs and Ephrins likely have other binding partners (Poliakov et al., 2004). Indeed, in culture, both EphA2 and EfnB1 have independently been shown to bind the tight junction protein claudin in cis, resulting in changes to cell adhesion (Tanaka et al., 2005a,b). In vivo, it has been demonstrated that EphA4 is constitutively associated with integrin in platelets (Prevost et al., 2005), while EfnB1 has been shown to bind Cx43, and thereby regulate gap junction formation and cell sorting in chimeric mice (Davy et al., 2006). Recently, EfnB1 has been shown to interact directly with Par6, a scaffolding protein essential for tight junction complex assembly; EfnB1 knock-down results in loss of tight junctions in *Xenopus* blastomeres (Lee et al., 2008). It is therefore possible that the regulation of cell adhesion by Ephs and Ephrins in the hindbrain neuroepithelium could be due to direct physical interaction with cell junction machinery at the cell surface.

Role of Ephs and Ephrins at other neuromere boundaries

Given that EphA4- and EfnB2a-based cell interactions in r3, r4 and r5 appears to maintain those rhombomere boundaries during neurulation, we hypothesize that there is a similar requirement for Ephs or Efns within r1,2,6, and 7. EfnB2a is also expressed in r1 and r7 and our data suggests that it promotes cell affinity there, although less robustly than in r4. As alluded to earlier, Eph and Ephrin candidates expressed in r2 and r6 include EfnB3 and EphB4a (Cooke et al., 2001; Cooke et al., 2005). Indeed, blocking Eph signaling in r6 prevented sorting-out of *mafB* mutant cells from r6 in genetic mosaics (Cooke et al., 2001). We do not see evidence for Eph- or Ephrin-based adhesion contributing to neuromere boundaries outside the hindbrain. Although EfnB2a is strongly expressed in the midbrain, EfnB2a MO cells do not sort out of the midbrain in mosaic embryos. We suggest that the control of neuroepithelial progenitor cell behaviour by Eph- and Ephrin-based adhesion is a unique attribute of the segmented hindbrain.

Relevance of Ephs and Ephrins to disease linked to mosaicism

Our insights into the role of EphA4 and EfnB2a in hindbrain development are based on the behaviour of cells in loss of function and gain of function EphA4 and EfnB2a mosaics and therefore may yield insights into diseases whose etiologies result from genetic mosaicism. Indeed, EfnB1-based mosaicism underlies the more severe cases of craniofrontonasal syndrome (CFNS) in humans and mice: females heterozygous for a mutation in the X-linked *EfnB1* gene exhibit symptoms not seen in hemizygous males or homozygous females due to sorting-out of EfnB1+ cell clones from EfnB1 mutant cell clones following random X-inactivation (Compagni et al., 2003; Davy et al., 2004; Twigg et al., 2004; Wieland et al., 2004).

A specific pathological example of mosaicism in the soma is cancer, in which cancerous cell clones, or tumours, arise that are genetically and behaviourly distinct from the surrounding tissue. We have described a role for EphA4 and EfnB2a in regulating cell sorting in the hindbrain neuroepithelium, and observe that small clones of cells exhibiting higher or lower levels of EphA4 or EfnB2a are segregated from the surrounding epithelium. In a similar way, EphB–EfnB interactions in the intestine normally mediate subtle cell positioning along the crypt-villus axis, but also play a dramatic role in compartmentalizing rare colorectal tumours, which appears to inhibit the onset of more aggressive forms of colon cancer (Cortina et al., 2007). It has been known for some time that Ephs and Ephrins are misregulated in many cancers and while the relationship remains poorly understood, it is clear that these molecules have important roles in a variety of "cancer mosaic" contexts (Clevers and Batlle, 2006; Merlos-Suarez and Batlle, in press; Pasquale, 2008). Abnormal levels of Eph or Ephrin on the surface of tumour cells may drive segregation of these cells from the surrounding healthy tissue, while at the same time mediating intra-tumour cell contacts. In these pathological

situations, the foci of abnormal Eph–Ephrin interactions arise sporadically and thus are difficult to study in situ. Understanding the cellular behaviours and molecular mechanisms underlying Eph- and Efn-based adhesive sorting in the teleost hindbrain may therefore shed light on cellular mechanisms underlying Eph- and Efn-dependent tumorigenesis.

Acknowledgments

We wish to thank colleagues who generously provided information, reagents, and transgenic lines: David Kimelman contributed the pHS-GFP-Tol2 vector backbone, Michael Brand and Alex Picker provided the pGFP5.3 line. We thank John Clarke for helpful comments on the timelapse movies. We also thank Paul Grant and Julio Vasquez for their help with confocal imaging, and Judy Bousman and Bobbie Schneider for epon sectioning of embryos. Finally, we wish to thank the members of the Moens lab for their thoughtful input into this project. The research was supported by National Institutes of Health grant HD37909 (C.B.M.). C.B.M. is an investigator with the Howard Hughes Medical Institute.

Appendix A. Supplementary data

Supplementary data associated with this article can be found, in the online version, at doi:10.1016/j.ydbio.2008.12.010.

References

Bergemann, A.D., Cheng, H.J., Brambilla, R., Klein, R., Flanagan, J.G., 1995. ELF-2, a new member of the Eph ligand family, is segmentally expressed in mouse embryos in the region of the hindbrain and newly forming somites. Mol. Cell. Biol. 15, 4921–4929.

Bong, Y.S., Park, Y.H., Lee, H.S., Mood, K., Ishimura, A., Daar, I.O., 2004. Tyr-298 in ephrinB1 is critical for an interaction with the Grb4 adaptor protein. Biochem. J. 377, 499–507.

Carmany-Rampey, A., Moens, C.B., 2006. Modern mosaic analysis in the zebrafish. Methods 39, 228–238.

Chan, J., Mably, J.D., Serluca, F.C., Chen, J.N., Goldstein, N.B., Thomas, M.C., Cleary, J.A., Brennan, C., Fishman, M.C., Roberts, T.M., 2001. Morphogenesis of prechordal plate and notochord requires intact Eph/ephrin B signaling. Dev. Biol. 234, 470–482.

Cheng, Y.C., Amoyel, M., Qiu, X., Jiang, Y.J., Xu, Q., Wilkinson, D.G., 2004. Notch activation regulates the segregation and differentiation of rhombomere boundary cells in the zebrafish hindbrain. Dev. Cell 6, 539–550.

Chenn, A., McConnell, S.K., 1995. Cleavage orientation and the asymmetric inheritance of Notch1 immunoreactivity in mammalian neurogenesis. Cell 82, 631–641.

Ciruna, B., Jenny, A., Lee, D., Mlodzik, M., Schier, A.F., 2006. Planar cell polarity signalling couples cell division and morphogenesis during neurulation. Nature 439, 220–224.

Clevers, H., Batlle, E., 2006. EphB/EphrinB receptors and Wnt signaling in colorectal cancer. Cancer Res. 66, 2–5.

Compagni, A., Logan, M., Klein, R., Adams, R.H., 2003. Control of skeletal patterning by ephrinB1–EphB interactions. Dev. Cell 5, 217–230.

Cooke, J., Moens, C., Roth, L., Durbin, L., Shiomi, K., Brennan, C., Kimmel, C., Wilson, S., Holder, N., 2001. Eph signalling functions downstream of Val to regulate cell sorting and boundary formation in the caudal hindbrain. Development 128, 571–580.

Cooke, J.E., Kemp, H.A., Moens, C.B., 2005. EphA4 is required for cell adhesion and rhombomere-boundary formation in the zebrafish. Curr. Biol. 15, 536–542.

Cortina, C., Palomo-Ponce, S., Iglesias, M., Fernandez-Masip, J.L., Vivancos, A., Whissell, G., Huma, M., Peiro, N., Gallego, L., Jonkheer, S., Davy, A., Lloreta, J., Sancho, E., Batlle, E., 2007. EphB–ephrin-B interactions suppress colorectal cancer progression by compartmentalizing tumor cells. Nat. Genet. 39, 1376–1383.

Cowan, C.A., Henkemeyer, M., 2001. The SH2/SH3 adaptor Grb4 transduces B-ephrin reverse signals. Nature 413, 174–179.

Davy, A., Aubin, J., Soriano, P., 2004. Ephrin-B1 forward and reverse signaling are required during mouse development. Genes Dev. 18, 572–583.

Davy, A., Bush, J.O., Soriano, P., 2006. Inhibition of gap junction communication at ectopic Eph/ephrin boundaries underlies craniofrontonasal syndrome. PLoS Biol. 4, e315.

Eberhart, J., Barr, J., O'Connell, S., Flagg, A., Swartz, M.E., Cramer, K.S., Tosney, K.W., Pasquale, E.B., Krull, C.E., 2004. Ephrin-A5 exerts positive or inhibitory effects on distinct subsets of EphA4-positive motor neurons. J. Neurosci. 24, 1070–1078.

Egea, J., Klein, R., 2007. Bidirectional Eph–ephrin signaling during axon guidance. Trends Cell. Biol. 17, 230–238.

Geldmacher-Voss, B., Reugels, A.M., Pauls, S., Campos-Ortega, J.A., 2003. A 90-degree rotation of the mitotic spindle changes the orientation of mitoses of zebrafish neuroepithelial cells. Development 130, 3767–3780.

Guthrie, S., Lumsden, A., 1991. Formation and regeneration of rhombomere boundaries in the developing chick hindbrain. Development 112, 221–229.

Guthrie, S., Prince, V., Lumsden, A., 1993. Selective dispersal of avian rhombomere cells in orthotopic and heterotopic grafts. Development 118, 527–538.

Hindges, R., McLaughlin, T., Genoud, N., Henkemeyer, M., O'Leary, D.D., 2002. EphB forward signaling controls directional branch extension and arborization required for dorsal–ventral retinotopic mapping. Neuron 35, 475–487.

Hirashima, M., Suda, T., 2006. Differentiation of arterial and venous endothelial cells and vascular morphogenesis. Endothelium 13, 137–145.

Holmberg, J., Clarke, D.L., Frisen, J., 2000. Regulation of repulsion versus adhesion by different splice forms of an Eph receptor. Nature 408, 203–206.

Itasaki, N., Sharpe, J., Morrison, A., Krumlauf, R., 1996. Reprogramming Hox expression in the vertebrate hindbrain: influence of paraxial mesoderm and rhombomere transposition. Neuron 16, 487–500.

Janes, P.W., Saha, N., Barton, W.A., Kolev, M.V., Wimmer-Kleikamp, S.H., Nievergall, E., Blobel, C.P., Himanen, J.P., Lackmann, M., Nikolov, D.B., 2005. Adam meets Eph: an ADAM substrate recognition module acts as a molecular switch for ephrin cleavage in trans. Cell 123, 291–304.

Kanda, T., Sullivan, K.F., Wahl, G.M., 1998. Histone-GFP fusion protein enables sensitive analysis of chromosome dynamics in living mammalian cells. Curr. Biol. 8, 377–385.

Kimmel, C.B., Warga, R.M., Kane, D.A., 1994. Cell cycles and clonal strings during formation of the zebrafish central nervous system. Development 120, 265–276.

Klein, R., 2004. Eph/ephrin signaling in morphogenesis, neural development and plasticity. Curr. Opin. Cell Biol. 16, 580–589.

Koshida, S., Kishimoto, Y., Ustumi, H., Shimizu, T., Furutani-Seiki, M., Kondoh, H., Takada, S., 2005. Integrinalpha5-dependent fibronectin accumulation for maintenance of somite boundaries in zebrafish embryos. Dev. Cell 8, 587–598.

Kwan, K.M., Fujimoto, E., Grabher, C., Mangum, B.D., Hardy, M.E., Campbell, D.S., Parant, J.M., Yost, H.J., Kanki, J.P., Chien, C.B., 2007. The Tol2kit: a multisite gateway-based construction kit for Tol2 transposon transgenesis constructs. Dev. Dyn. 236, 3088–3099.

Lee, H.S., Nishanian, T.G., Mood, K., Bong, Y.S., Daar, I.O., 2008. EphrinB1 controls cell–cell junctions through the Par polarity complex. Nat. Cell Biol. 10, 979–986.

Lu, Q., Sun, E.E., Klein, R.S., Flanagan, J.G., 2001. Ephrin-B reverse signaling is mediated by a novel PDZ-RGS protein and selectively inhibits G protein-coupled chemoattraction. Cell 105, 69–79.

Makinen, T., Adams, R.H., Bailey, J., Lu, Q., Ziemiecki, A., Alitalo, K., Klein, R., Wilkinson, G.A., 2005. PDZ interaction site in ephrinB2 is required for the remodeling of lymphatic vasculature. Genes Dev. 19, 397–410.

Marston, D.J., Dickinson, S., Nobes, C.D., 2003. Rac-dependent trans-endocytosis of ephrinBs regulates Eph–ephrin contact repulsion. Nat. Cell Biol. 5, 879–888.

McLaughlin, T., Hindges, R., Yates, P.A., O'Leary, D.D., 2003. Bifunctional action of ephrin-B1 as a repellent and attractant to control bidirectional branch extension in dorsal–ventral retinotopic mapping. Development 130, 2407–2418.

Megason, S.G., Fraser, S.E., 2003. Digitizing life at the level of the cell: high-performance laser-scanning microscopy and image analysis for in toto imaging of development. Mech. Dev. 120, 1407–1420.

Mellitzer, G., Xu, Q., Wilkinson, D.G., 1999. Eph receptors and ephrins restrict cell intermingling and communication. Nature 400, 77–81.

Merlos-Suarez, A., Batlle, E., In Press., Eph–ephrin signalling in adult tissues and cancer. Curr. Opin. Cell Biol. 20, 194–200.

Moens, C.B., Yan, Y.L., Appel, B., Force, A.G., Kimmel, C.B., 1996. valentino: a zebrafish gene required for normal hindbrain segmentation. Development 122, 3981–3990.

Nieto, M.A., Gilardi-Hebenstreit, P., Charnay, P., Wilkinson, D.G., 1992. A receptor protein tyrosine kinase implicated in the segmental patterning of the hindbrain and mesoderm. Development 116, 1137–1150.

Oxtoby, E., Jowett, T., 1993. Cloning of the zebrafish krox-20 gene (krx-20) and its expression during hindbrain development. Nucleic Acids Res. 21, 1087–1095.

Palmer, A., Zimmer, M., Erdmann, K.S., Eulenburg, V., Porthin, A., Heumann, R., Deutsch, U., Klein, R., 2002. EphrinB phosphorylation and reverse signaling: regulation by Src kinases and PTP-BL phosphatase. Mol. Cell 9, 725–737.

Papan, C., Campos-Ortega, J.A., 1999. Region-specific cell clones in the developing spinal cord of the zebrafish. Dev. Genes Evol. 209, 135–144.

Pasquale, E.B., 2008. Eph–ephrin bidirectional signaling in physiology and disease. Cell 133, 38–52.

Picco, V., Hudson, C., Yasuo, H., 2007. Ephrin–Eph signalling drives the asymmetric division of notochord/neural precursors in *Ciona* embryos. Development 134, 1491–1497.

Picker, A., Scholpp, S., Bohli, H., Takeda, H., Brand, M., 2002. A novel positive transcriptional feedback loop in midbrain–hindbrain boundary development is revealed through analysis of the zebrafish pax2.1 promoter in transgenic lines. Development 129, 3227–3239.

Poliakov, A., Cotrina, M., Wilkinson, D.G., 2004. Diverse roles of eph receptors and ephrins in the regulation of cell migration and tissue assembly. Dev. Cell 7, 465–480.

Prevost, N., Woulfe, D.S., Jiang, H., Stalker, T.J., Marchese, P., Ruggeri, Z.M., Brass, L.F., 2005. Eph kinases and ephrins support thrombus growth and stability by regulating integrin outside-in signaling in platelets. Proc. Natl. Acad. Sci U. S. A. 102, 9820–9825.

Prince, V.E., Moens, C.B., Kimmel, C.B., Ho, R.K., 1998. Zebrafish hox genes: expression in the hindbrain region of wild-type and mutants of the segmentation gene, valentino. Development 125, 393–406.

Reid, C.B., Tavazoie, S.F., Walsh, C.A., 1997. Clonal dispersion and evidence for asymmetric cell division in ferret cortex. Development 124, 2441–2450.

Roszko, I., Afonso, C., Henrique, D., Mathis, L., 2006. Key role played by RhoA in the balance between planar and apico-basal cell divisions in the chick neuroepithelium. Dev. Biol. 298, 212–224.

Santiago, A., Erickson, C.A., 2002. Ephrin-B ligands play a dual role in the control of neural crest cell migration. Development 129, 3621–3632.

Schilling, T.F., Prince, V., Ingham, P.W., 2001. Plasticity in zebrafish hox expression in the hindbrain and cranial neural crest. Dev. Biol. 231, 201–216.
Sela-Donenfeld, D., Wilkinson, D.G., 2005. Eph receptors: two ways to sharpen boundaries. Curr. Biol. 15, R210–212.
Tanaka, M., Kamata, R., Sakai, R., 2005a. EphA2 phosphorylates the cytoplasmic tail of Claudin-4 and mediates paracellular permeability. J. Biol. Chem. 280, 42375–42382.
Tanaka, M., Kamata, R., Sakai, R., 2005b. Phosphorylation of ephrin-B1 via the interaction with claudin following cell–cell contact formation. EMBO J. 24, 3700–3711.
Tawk, M., Araya, C., Lyons, D.A., Reugels, A.M., Girdler, G.C., Bayley, P.R., Hyde, D.R., Tada, M., Clarke, J.D., 2007. A mirror-symmetric cell division that orchestrates neuroepithelial morphogenesis. Nature 446, 797–800.
Torres, R., Firestein, B.L., Dong, H., Staudinger, J., Olson, E.N., Huganir, R.L., Bredt, D.S., Gale, N.W., Yancopoulos, G.D., 1998. PDZ proteins bind, cluster, and synaptically colocalize with Eph receptors and their ephrin ligands. Neuron 21, 1453–1463.
Twigg, S.R., Kan, R., Babbs, C., Bochukova, E.G., Robertson, S.P., Wall, S.A., Morriss-Kay, G.M., Wilkie, A.O., 2004. Mutations of ephrin-B1 (EFNB1), a marker of tissue boundary formation, cause craniofrontonasal syndrome. Proc. Natl. Acad. Sci. U. S. A. 101, 8652–8657.
Wallingford, J.B., 2005. Neural tube closure and neural tube defects: studies in animal models reveal known knowns and known unknowns. Am. J. Med. Genet. C Semin. Med. Genet. 135C, 59–68.
Waskiewicz, A.J., Rikhof, H.A., Moens, C.B., 2002. Eliminating zebrafish pbx proteins reveals a hindbrain ground state. Dev. Cell 3, 723–733.
Westerfield, M., 1993. The Zebrafish Book; A Guide for the Laboratory Use of Zebrafish (*Brachydanio rerio*). University of Oregon Press, Eugene.
Wieland, I., Jakubiczka, S., Muschke, P., Cohen, M., Thiele, H., Gerlach, K.L., Adams, R.H., Wieacker, P., 2004. Mutations of the ephrin-B1 gene cause craniofrontonasal syndrome. Am. J. Hum. Genet. 74, 1209–1215.
Xu, Q., Mellitzer, G., Robinson, V., Wilkinson, D.G., 1999. In vivo cell sorting in complementary segmental domains mediated by Eph receptors and ephrins. Nature 399, 267–271.
Zimmer, M., Palmer, A., Kohler, J., Klein, R., 2003. EphB–ephrinB bi-directional endocytosis terminates adhesion allowing contact mediated repulsion. Nat. Cell Biol. 5, 869–878.